J Braz. Soc. Mech. Sci. Eng. (2017) 39:401–412
DOI 10.1007/s40430-016-0489-7

TECHNICAL PAPER

Analytical modeling for perforation of foam-composite sandwich panels under high-velocity impact

S. Feli[1] · **S. S. Jafari**[1]

Received: 14 December 2014 / Accepted: 11 January 2016 / Published online: 21 January 2016

Abstract In this paper, a new simple analytical model for perforation process of composite sandwich panels subjected to high-velocity impact of flat-ended projectile is presented. The panels consist of foam core sandwiched between two composite skins. In the analytical model, global deformation, plug shearing or localized tensile fracture, delamination of front and back-up composite skins, and the absorbed energy during the perforation of the sandwich panel are calculated considering the local indentation and also the energy balancing equation is employed to determine the ballistic limit and residual velocity of projectile. The results of current new model are compared with the experimental results available in the open literature and the finite element simulation results obtained by the LS-Dyna code. A good agreement is observed between the analytical and numerical model results and the experimental results.

Keywords Fibers · Foam · Impact behavior · Analytical modeling · Numerical analysis

1 Introduction

Foam-composite sandwich panels have received several attentions over the past few years and they are now the first choice for fabricating structures where low weight in combination with the high strength and stiffness is required. Foam-composite sandwich panels have great commercial application. They are extensively used in aerospace, automotive, marine, and construction industries due to their inherent advantages over the conventional metals.

Over the past recent decades, many researchers have focused on the experimental and theoretical investigations of the transverse impact response of polymer matrix composite laminates in order to gain their failure, energy absorption mechanisms, and the ballistic impact behavior of composites.

Ulven et al. [1] investigated the perforation, energy absorption, damage evolution, and ballistic limit velocity on the carbon/epoxy laminates that struck by various projectiles experimentally and analytically. Wen [2] studied the penetration and perforation of FRP (Fiber-Reinforced Plastic) laminates using different projectile shapes in the high-velocity impact and also he proposed analytical equations to predict the depth of penetration and ballistic limit velocity. In addition, Wen [3] displayed the penetration and perforation of thick FRP laminates that struck considering different ended projectiles.

Naik et al. [4] presented a new analytical method based on the wave theory for ballistic impact on woven fabric composite. They identified different damage and energy absorbing mechanisms including cone formation on the back face of target, tension in the primary yarns, deformation of secondary yarns, delamination, matrix cracking, shear plugging, and friction during penetration. Feli and Asgari [5] developed a new technique for normal penetration of cylindrical projectiles onto the ceramic-composite targets based on the F.E. simulation using LS-Dyna code.

López-Puente et al. [6] employed an analytical model to predict the residual velocity of a cylindrical steel projectile,

Technical Editor: Fernando Alves Rochinha.

✉ S. S. Jafari
sjd.jafari@yahoo.com

S. Feli
Felisaeid@razi.ac.ir

[1] Department of Mechanical Engineering, Razi University, P.O. BOX: 67149-67346, Kermanshah, Islamic Republic of Iran

after impacting into a woven carbon/epoxy thin laminate. Their model was based on the energy balance, in which the laminate absorbed the kinetic projectile energy through the three different mechanisms including, linear momentum transfer, fiber failure, and laminate crushing.

Mamivand and Liaghat [7] developed an analytical model for the ballistic behavior of two-dimensional woven fabric composites. Their model developed the penetration process of cylindrical projectile based on the conservation of momentum and wave theory.

Feli et al. [8] demonstrated the perforation of ceramic/multi-layer woven fabric targets by blunt projectiles analytically. In their model, the kinetic and strain energy of yarns were determined for modeling the back-up woven-fabric material and deformation of yarns during perforation.

The influence of the honeycomb core on the stiffness, damage, and penetration resistance of sandwich panel under high- and low-velocity impacts was widely studied. Hoo Fatt and Park [9] presented an analytical solution for the ballistic limit of a sandwich honeycomb panels subjected to the normal impact by the blunt and spherical projectiles. Their used sandwich honeycomb panel consisted of a honeycomb core with the thin top and the bottom metallic facesheets. Their solution involved a three-stage perforation process including, perforation of the top facesheet, honeycomb core, and the bottom facesheet.

Feli and Namdari pour [10] developed an analytical model for the composite sandwich panels with the honeycomb core subjected to the high-velocity impact. In their model, perforation of panel was studied in three stages: perforation of top skin, perforation of honeycomb, and perforation of bottom skin.

Lin and Hoo Fatt [11] applied an analytical model for deformation, penetration, and perforation of the composite plate and composite sandwich panels with honeycomb core subjected to the quasi-static punch indentation and projectile impact. The value of ballistic limit velocity for E-glass/epoxy-aluminum honeycomb sandwich was impacted by hemispherical nose projectile, obtained by a quasi-static impact model.

Xie et al. [12] investigated the local indentation response of sandwich panels with the metallic foam core under a flat-spherical indenter via analytical and numerical model. The ABAQUS code was also used to simulate this process.

The analysis of sandwich panels with the composite face sheets and polymer foam, investigated in the current paper, is complex and hence has not been treated analytically by previous researchers. Hoo Fatt and Sirivolu [13], Wen et al. [14], and Reddy et al. [15] analytical models' have been developed to describe this system so far.

Hoo Fatt and Sirivolu [13] presented a model for high-velocity impact on the composite sandwich panel. Their model was based on the wave propagation model. They used a lagrangian mechanics to derive the equation of projectile motion.

Wen et al. [14] studied the indentation and perforation of composite laminates and composite-foam sandwich panel experimentally. They used projectiles with different shapes (flat-ended, hemispherical-nosed, and conical-nosed). In addition, Reddy et al. [15] investigated the penetration of hemispherical- and conical-nosed projectile into the composite-foam sandwich panel by empirical formulas. They considered the local and global deformation to determine the absorbed energy by panel.

The objective of this paper is to develop a new simple analytical model for perforation process of composite sandwich panels with the foam core subjected to the high-velocity impact of flat-ended projectile. New model for the global deformation with the local rupture of front and back-up composite skins is also presented. The ballistic limit and residual velocity of projectile has been determined by computing the energy absorbed by composite skins and foam core and using the energy balance equation. In addition, a three-dimensional, dynamic-explicit, Lagrangian method is used in LS-Dyna code for the F.E. simulation of perforation process. The model is also validated by comparing the Wen [14] experimental test results and F.E. simulation results via LS-Dyna code. In addition, the effects of projectile mass and diameter in energy absorption of sandwich panel are investigated.

2 Analytical model

Consider a sandwich composite-foam panel impacted by the flat-ended projectile, as shown in Fig. 1. The composite sandwich panel with foam core consists of a foam core sandwiched between two FRP composite skins. The thickness of foam core and composite skins is c and h, respectively. The projectile shape is cylindrical, with the radius R_p, mass M_p, and initial velocity V_0. The panel-absorbed energy consists of the energy absorbed by composite skins and energy absorbed by the foam core.

2.1 Energy absorbed by composite skins

Wu et al. [16] developed an analytical model for perforation of FRP laminate contained two failure modes including the global deformation with local rupture and wave-dominated with local response. The ballistic limit velocity is obtained from energy balance so that the kinetic energy of projectile is absorbed by FRP laminate. In this paper, we only consider the global deformation with local rupture of laminates during perforation.

The kinetic energy of projectile is absorbed by the laminate through the local indentation, global deformation,

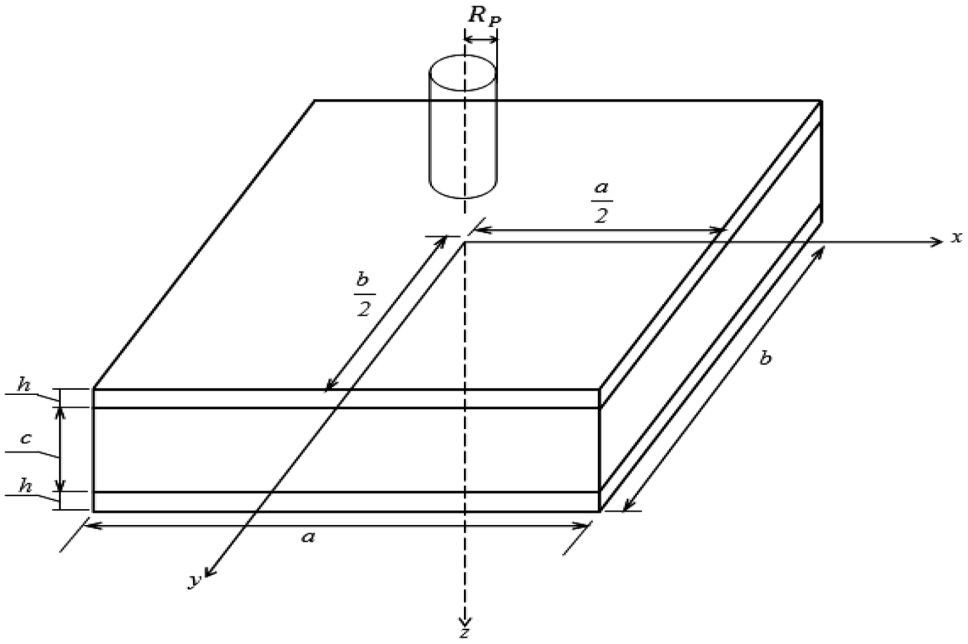

Fig. 1 Description of impact loading on composite-foam sandwich panel

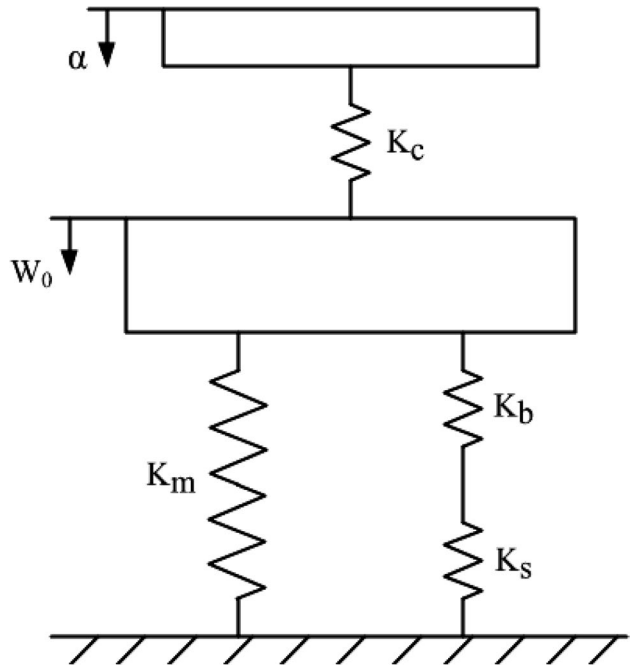

Fig. 2 The spring-mass model [13]

shearing plugging, localized tensile fracture, or delamination. Impact perforation energy is obtained by the quasi-static energy multiplied by a dynamic enhancement factor.

Quasi-static loading on the FRP laminate using spring-mass model has been shown in Fig. 2. The laminate deformation contains local indentation, global bending, and stretching.

The quasi-static contact force (P) is related to the local indentation of the laminate plate (α), as [14]

$$P = K_c \alpha \tag{1}$$

where K_c indicates the contact stiffness and defines by the following equation:

$$K_c = \frac{D_p}{\pi H_0} \tag{2}$$

where D_p is the diameter of indenter and H_0 is defined as [14]

$$H_0 = \frac{(\gamma_1 + \gamma_2) C_{11}}{2\pi (C_{11} C_{33} - C_{13}^2)}, \quad \gamma_{1,2}^2 = Q \pm \sqrt{Q^2 - C_{33}/C_{11}},$$

$$Q = (C_{11} C_{33} - C_{13}^2 - 2C_{13} C_{44}) \Big/ 2C_{11} C_{44}$$

In the above equation C_{ij} indicates the elastic constants for transversely isotropic elastic body.

The load (P) and transverse deflection of the mid-plane (W_0) are related by:

$$P = K_{bs} W_0 + K_m W_0^3 \tag{3}$$

where K_{bs} and K_m are the effective stiffness due to bending and shear and the membrane stiffness, respectively. In Eq. (3), the local indentation is ignored. For the square fully clamped plate, K_b and K_m are given by the following equations [14, 17]:

$$K_b = \frac{16\pi E_1 h^3}{3(1 - \upsilon_{12}^2) S^2} \tag{4}$$

$$K_m = \frac{191\pi E_1 h}{162 S^2} \tag{5}$$

where E_1 and υ_{12} are the in-plane Young's module and the poison's ratio, and also h and S are the laminate thickness and span of the laminate plate, respectively.

The effective shear stiffness is presented as [17]:

$$K_s = \frac{4\pi}{3} G_{13} h \left(\frac{E_1}{E_1 - 4\upsilon_{12} G_{13}} \right) \left(\frac{4}{3} + Log \frac{S}{2R_p} \right)^{-1} \quad (6)$$

where G_{13} is the shear module. Considering Fig. 2, the effective stiffness due to bending and shear is obtained using the bellow equation:

$$\frac{1}{K_{bs}} = \frac{1}{K_b} + \frac{1}{K_s} \quad (7)$$

By experimental observation, the FRP laminate absorbs energy by local indentation, global deformation, shearing plugging, localized tensile fracture, or delamination. The total energy due to deformation (E_{def}) can be written as [16]:

$$E_{def} = \left[\frac{(K_{bs} W_{0f} + K_m W_{0f}^3)^2}{2K_c} \right] + \left[\frac{1}{2} K_{bs} W_{0f}^2 + \frac{1}{4} K_m W_{0f}^4 \right] \quad (8)$$

where W_{0f} is the critical transverse deflection in which plate failure occurs. The first and the last terms on the right hand side of Eq. (8) are the energy absorbed by the local indentation and the energy absorbed by the global deformation, respectively.

The quasi-static contact load (P), critical transverse deflection (W_{0f}), and the transverse shear strength of the laminate plate (τ_{13}) are related together using an equation of the following form [14]:

$$P = K_{bs} W_{0f} + K_m W_{0f}^3 = 2\pi R_p h K \tau_{13} \quad (9)$$

where K is a constraint factor. For simplicity K is taken as 2 [14].

According to experimental observation, failure of FRP laminate plate loaded by a flat-ended punch depends on the ratio of plate thickness to punch diameter (h/D_p). When h/D_p is smaller than a critical value (ϕ), the plate will fail by the local shear plugging; otherwise it will fail by the mixed mode of local shear and tensile tearing. Hence, the energy dissipated by the local failure (E_{frac}) can be obtained by the following equation:

$$E_{frac} = \pi R_p h^2 K \tau_{13} \quad \text{for } h/D_p > \phi \quad (10)$$

$$E_{frac} = \pi R_p^2 (h - \phi D_p) e_t + \pi R_p (\phi D_p)^2 K \tau_{13} \quad \text{for } h/D_p > \phi \quad (11)$$

where e_t is the energy density for tensile tearing failure and ϕ is an empirical constant which can be taken equal to 0.21 approximately [16].

Delamination initiates below the contact loading area by coalescence of matrix cracks at interfaces with high inter-laminar shear stresses. The energy due to delamination (E_{del}) can be expressed as [16]:

$$E_{del} = \frac{9}{16\pi h^2} \left(\frac{P_d}{\tau_{IRSS}} \right)^2 G_{IIC} \quad (12)$$

where G_{IIC} and τ_{IRSS} are the inter-laminar fracture toughness in mode II and the inter-laminar shear stress, respectively. The critical indenter load delamination (P_d) can be obtained using the following equation [18]:

$$P_d^2 = \frac{8\pi^2 E_1 h^3 G_{IIC}}{9(1 - \upsilon_{12}^2)} \quad (13)$$

The total energy (E_{scom}), dissipated in the perforation of an FRP laminate plate loaded quasi-statically by a flat indenter at the center, can be therefore written as:

$$E_{scom} = E_{def} + E_{frac} + E_{del} \quad (14)$$

For evaluating the impact perforation energy (E_P), dynamic enhancement factor (φ) is employed. The impact perforation energy can be expressed by the following equation:

$$E_{dcom} = \varphi E_{scom} \quad (15)$$

The dynamic enhancement factor may be expressed as [14]:

$$\varphi = \begin{cases} 1 + B\left(\frac{V_i}{V_c}\right) & (V_i < V_c) \\ 1 + B\left(\frac{V_i}{V_c}\right) & (V_i > V_c) \end{cases} \quad (16)$$

where B, V_i, and V_c are an empirical constant, initial impact velocity of the projectile, and the Von Karman critical impact velocity, respectively. Also V_c is given as follows [14]:

$$V_c = \sqrt{\frac{E_1}{\rho_t}} \varepsilon_f \quad (17)$$

In Eq. (17), ε_f is the static tensile failure strain. ρ_t and E_1 are the density and in-plane Young's modulus of the laminates.

2.2 Energy absorbed by foam core

The sandwich panel core absorbs a part of initial kinetic energy of projectile. According to experimental observations, a part of projectile kinetic energy dissipates by foam crushing. The foam-energy absorbed can be obtained by [19]:

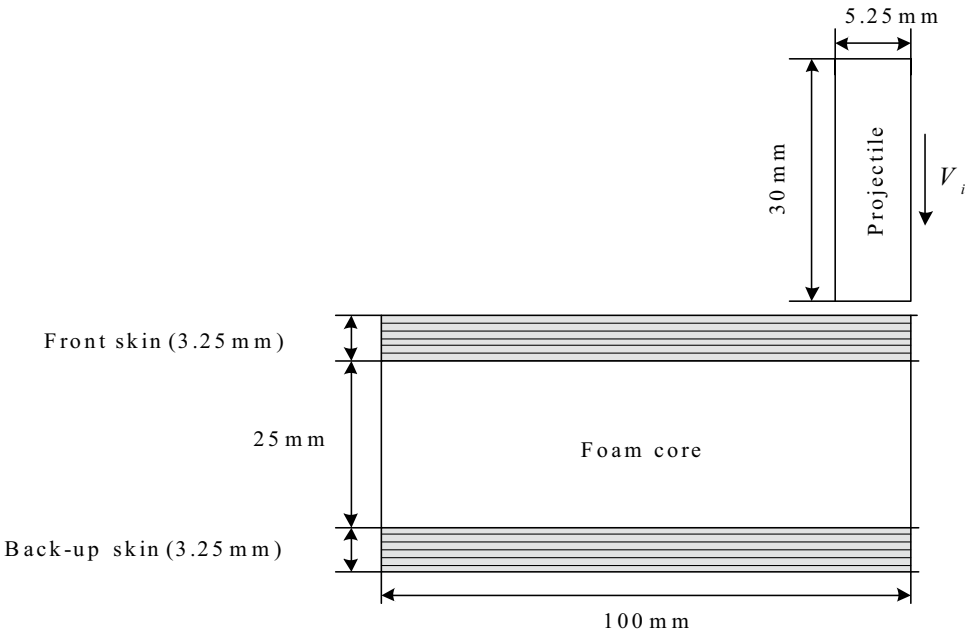

Fig. 3 The 2D axi-symmetric model of projectile and foam-composite sandwich panel

$$E_{\text{sfoam}} = \frac{\pi}{4} KD^2 c\varepsilon_{\text{d}}\sigma_{\text{c}} \tag{18}$$

where c is the core thickness. Also ε_{d} and σ_{c} are the densification and compressive strength of foam core, respectively.

The foam-energy absorbed in the dynamic loading is equal to:

$$E_{\text{dfoam}} = \varphi E_{\text{sfoam}} \tag{19}$$

2.3 Energy absorbed by sandwich panel

If the composite skins fail by the global deformation, the energy absorbed by the sandwich panel can be computed from the following equation:

$$E_{\text{T}} = 2E_{\text{dcom}} + E_{\text{dfoam}} \tag{20}$$

An approximate value for the ballistic limit velocity (V_{b}) is obtained by:

$$V_{\text{b}} = \sqrt{\frac{2E_{\text{T}}}{M_{\text{P}}}} \tag{21}$$

Also by using the energy balance equation, residual velocity of projectile can be determined as:

$$V_{\text{r}} = \sqrt{V_i^2 - V_{\text{b}}^2} \tag{22}$$

3 F.E. modeling description

The three-dimensional, Lagrangian, dynamic-explicit, and nonlinear analysis has been utilized for F.E. simulation of perforation process. For simplicity, a quadratic of sandwich panel is simulated. Geometric dimensions of sandwich panel and blunt projectile are shown in Fig. 3. Front and back-up composite skins are composed of six cross-ply laminates.

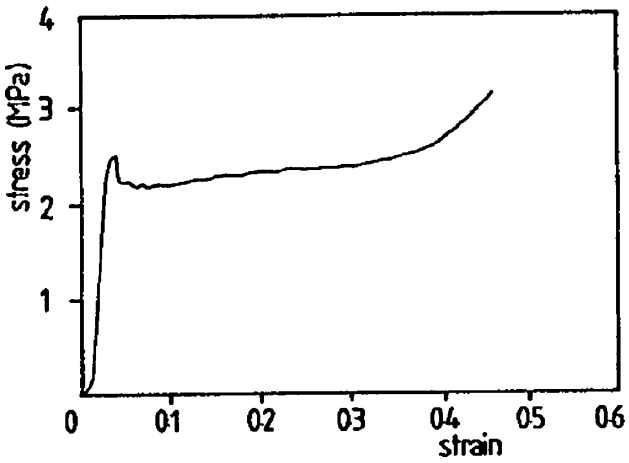

Fig. 4 Stress–strain curve of Divinycell H130 foam [13]

The cylindrical steel projectile of 10.5 mm in diameter, 30 mm length, and 20.4 g in mass has been used in FE simulation. The MAT_RIGID and MAT_CRUSHABLE_FOAM models in LS-Dyna code have been chosen to model the projectile and foam core, respectively. The stress–strain curve of Divinycell H130 foam is shown in Fig. 4.

In addition, the Composite-Damage material behavior has been considered for simulation of FRP laminates. This model is based on the Chang–Chang criterion, which

Table 1 Mechanical properties of Composite- Damage Model of E-Glass/Polyester [13] used in LS-Dyna F.E. simulation

Young's modulus (GPa)			Density ρ (g/cm^3)	Type	
E_1	E_2	E_3			
24	24	10.56	1.65	E-glass/polyester	
Shear modulus (GPa)			Poison ratio		
G_{12}	G_{13}	G_{23}	v_{12}	v_{13}	v_{23}
4	1.8	1.8	0.15	0.12	0.12
Shear strength S_{12} (GPa)	Longitudinal tensile strength S_1 (GPa)	Normal tensile strength S_N	Transverse tensile strength S_2 (GPa)	Transverse compressive strength C_2 (GPa)	Nonlinear parameters of shear stress α
0.0511	0.345	0.036	0.345	0.2552	0

Table 2 Material erosion parameters for foam core and composite skins used for erosive simulations in LS-Dyna code

Parameter	Notation	Composite skin	Dinavill cell H130 foam
Inelastic deactivation strain for erosive simulations (%)	EPSP1	9	–
Principal stress at failure (MPa)	SIGP1	–	2.5

contains three failure criteria [20]. Failure of composite is deemed to occur when the combined stresses reach a critical value. It may result from fiber fracture, matrix cracking, or compressive failure.

Composite material has anisotropic behavior; their thermo-elastic properties along and transverse to the fiber axis are different. These fibers are considered to be transversely isotropic, and thus five independent constants are needed to describe their properties, namely E_{1f}, E_{2f}, G_{12f}, v_{12f}, and G_{23f} [20]. The following expressions describe the elastic properties of a unidirectional lamina composed to anisotropic fibers in an isotropic matrix.

$$E_1 = E_{f1}V_f + E_m V_m, \quad E_2 = E_3 = \frac{E_m}{1 - V_f(1 - E_m/E_{f2})}$$
$$G_{12} = G_{13} = \frac{G_m}{1 - V_f(1 - G_m/G_{f12})}, \quad G_{23}\frac{G_m}{1 - V_f(1 - G_m/G_{f23})}$$
$$v_{12} = v_{13} = v_{f12}V_f + v_m V_m, \quad v_{23} = \frac{\frac{v_{f23}}{E_{f2}} + \frac{v_m}{E_m}}{\frac{V_f}{E_{f2}} + \frac{V_m}{E_m}} \tag{23}$$

In the above equations, the index "f" refers to the fiber and "m" refers to matrix of composite material. From the mechanical properties of fibers and matrix, the elastic constants in the above equations are listed in Table 1.

The material behavior models used in F. E. simulation of failed elements are not deleted from the computation. Thus, the distortions due to large deformations of elements will drastically reduce the time step size needed to find a stable solution of the governing equations that will either stop computations or make them progress extremely slowly. This overcomes by using the failure model Mat-add-erosion, regarding the material in an element to have failed with defined maximum principal strain and deleting the failed element from the calculation.

In this paper, the material erosion parameters for foam and composite materials have been considered for erosive simulations. Material erosion parameters are presented in Table 2.

The mesh scheme for the projectile, foam, and composite layers is shown in Fig. 5. A three-dimensional quadratic solid element with 8 nodes has been used.

The "ERODING_SINGLE_SURFACE (SOFT = 2)" option has been used for all contact surfaces during the perforation process. In high-velocity impact problem, the effect of frictional forces on the interfaces is negligible. In this, simulating static friction and dynamic friction are equal to 0.3 and 0.28, respectively [5].

4 Results and discussion

4.1 Validation of model

The validity of the present analytical model and F.E. simulation is assessed with the results available from the other references. The results of the analytical and F.E. models are compared with the experimental test results of Wen et al. [14]. The flat-ended cylindrical projectile was made of steel with the diameter 10.5 mm and mass 20.4 g [14]. The composite sandwich panel has composed of Woven Roving E-Glass/Polyester as a front and back-up composite skins and the PVC foam core is Divinycell H130.

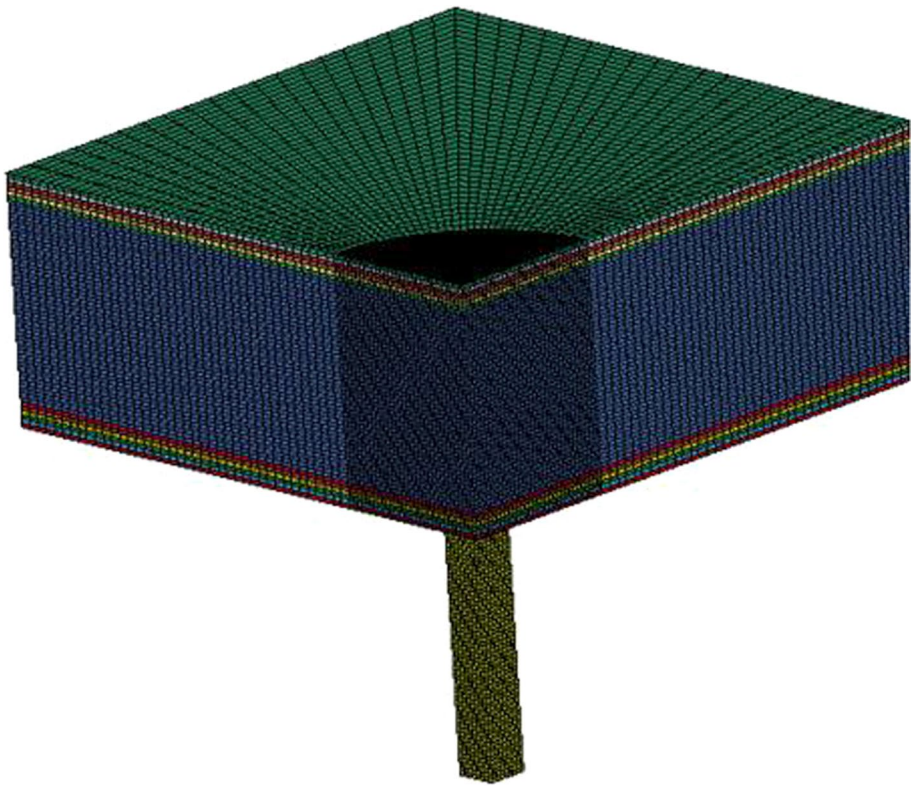

Fig. 5 Mesh scheme for the projectile, foam and composite layers in 3D F.E. simulation in LS-Dyna code

Table 3 Material parameters for E-glass/epoxy and carbon/epoxy composite skins [1, 13] used in new analytical model

Parameter	Notation	E-glass/epoxy	Carbon/epoxy
Density (kg/m^3)	ρ	1650	1550
In-plane Young's moduli (GPa)	E_{s1}	24	53.7
Through-thickness Young's moduli (GPa)	E_3	6.87	11.7
Shear modulus (GPa)	G_{st}	1.8	4
Poison ratio	ν_{12}	0.15	0.31
Transverse shear strength of plate (MPa)	τ_{13}	45	79
Energy density for tensile tearing failure (MJ/m^3)	e_t	4.23	5.1
Inter-laminar shear stress (MPa)	τ_{IRSS}	13	50
Inter-laminar fracture toughness in Mode II (KJ/m^2)	G_{IIC}	2.8	0.8
Static tensile failure strain	ε_f	0.021	0.0138

Table 4 Material parameters for Divinycell H130 foam [13]

Parameter	Notation	Value
Density (kg/m^3)	ρ	170
Young's moduli (GPa)	E	0.175
Densification strain	ε_d	0.45
Compressive strength (MPa)	σ_c	2.5

The mechanical properties of composite skin and foam core are given in Tables 3 and 4, respectively [1, 13].

The ballistic limit velocity of projectile computed by the new model has been compared with the experimental results [14] for different (H/D) in Fig. 6, where H is the total thickness of sandwich panel. The mass and diameter of projectile are equal to 20.4 g and 10.5 mm, respectively. Also, panel span and foam thickness are equal to 200 and 25 mm. The front and back-up skin thicknesses increase and the foam thickness remains constant. A good agreement between the ballistic limit velocity of projectile in the new model and Wen et al. [14] experimental test results has been observed.

The residual velocity of projectile predicted by the new model has been compared with the experimental results of Ref. [14] for three different thicknesses of front and back-up laminate skins in Fig. 7. The sandwich panel span and

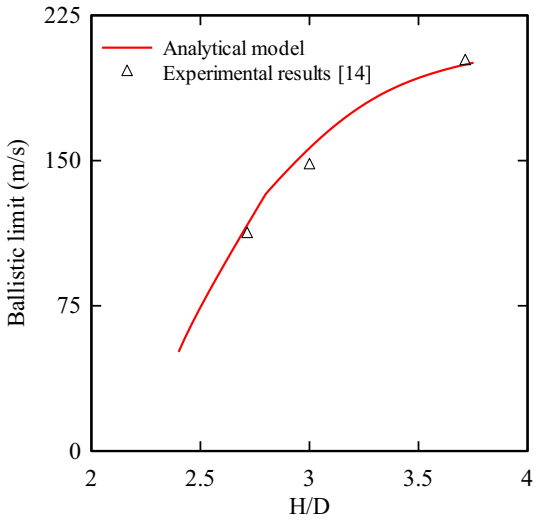

Fig. 6 Ballistic limit velocity versus total thickness of panel to projectile diameter and comparison analytical model with experimental results [13]

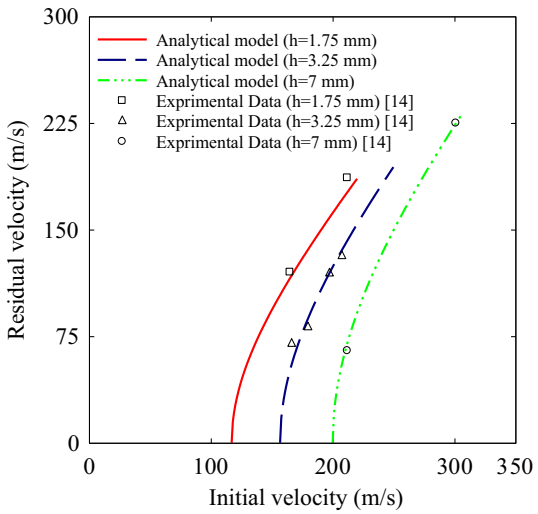

Fig. 7 Residual velocity versus initial velocity of projectile and comparison analytical model with experimental results [13]

foam core thickness are equal to 200 and 25 mm that struck by 10.5 mm diameter and 20.4 g mass flat-ended projectile. According to this figure, the ballistic limit velocity of projectile estimated by the new model is in consistence with the experimental results for different thicknesses of front and back-up skins. With an increase in front and back-up skin thickness, the residual velocity of projectile decreases.

The process of projectile penetration in the sandwich panel at LS-Dyna simulation is illustrated in Fig. 8. The initial velocity of projectile is 197.04 m/s. The perforation time is 0.2 ms and the residual velocity of projectile is 140.17 m/s.

In Fig. 9, the velocity–time history of projectile predicted by LS-Dyna simulation has been shown. The initial velocity of projectile is 197.04 m/s. The decreasing of projectile velocity during perforation of front and back-up composite skins (stage 1 and 3) is higher than that of foam core. Based on the results of new model for impact velocity 197.04 m/s, the projectile loses 32.75 % of its initial kinetic energy. Also the front and back-up composite skins and foam core decrease 17.12, 1.83, and 17.34 % of the projectile initial velocity, respectively. Therefore, the front and back-up composite skins are the main factor responsible for the energy adsorption, while the energy absorbed by the foam core is much lower.

Figure 10 presents a comparison between the results of residual velocity computed by the new model and the LS-DYNA F.E. simulations and experimental results [14] for sandwich panel with E-glass/epoxy composite skins and Divinycell H130 foam. In addition, because of the wide application of carbon/epoxy composite in aerospace industrial, in Fig. 11, the residual velocity of projectile computed by new model has been compared with the residual velocity determined by LS-DYNA F.E. simulation. The sandwich panel consists of the carbon/epoxy composite skins and Divinycell H130 foam. In these figures, the thicknesses of composite skins are equal to 3.25 mm. These laminates struck by a 20.4 g mass and 10.5 mm diameter flat-nosed projectile. It is evident from Fig. 10 that a good agreement between the residual velocity of projectile in the new analytical model and the experimental test results of Ref. [14] is observed and also the prediction of residual velocity of new analytical model is seemed to be better than the LS-Dyna F. E. simulation. In addition, by comparing the results of Figs. 10 and 11, it is clear that residual velocity in carbon/epoxy skin is greater than E-glass/epoxy skin at the same condition.

In the new F.E. simulation, presented in this paper, the Composite-Damage model, which determines the failure of composite under the fiber fracture, matrix cracking or compressive failure has been used for material behavior of composite material. However, the strain-rate effect has been ignored in stress–strain relationship of yarns. The coefficients of mechanical properties in Composite- Damage model, chosen for FRP laminates, have been selected from Lin and Hoo Fatt [11].

4.2 Parametric study of new model

In this section, the effects of projectile diameter and mass on the ballistic limit, residual velocity of projectile and the energy absorption of composite-foam sandwich panel have been investigated. Figure 12 depicts the ballistic limit velocity versus the diameter of projectile (D) for different projectile masses. In this figure, panel span, composite

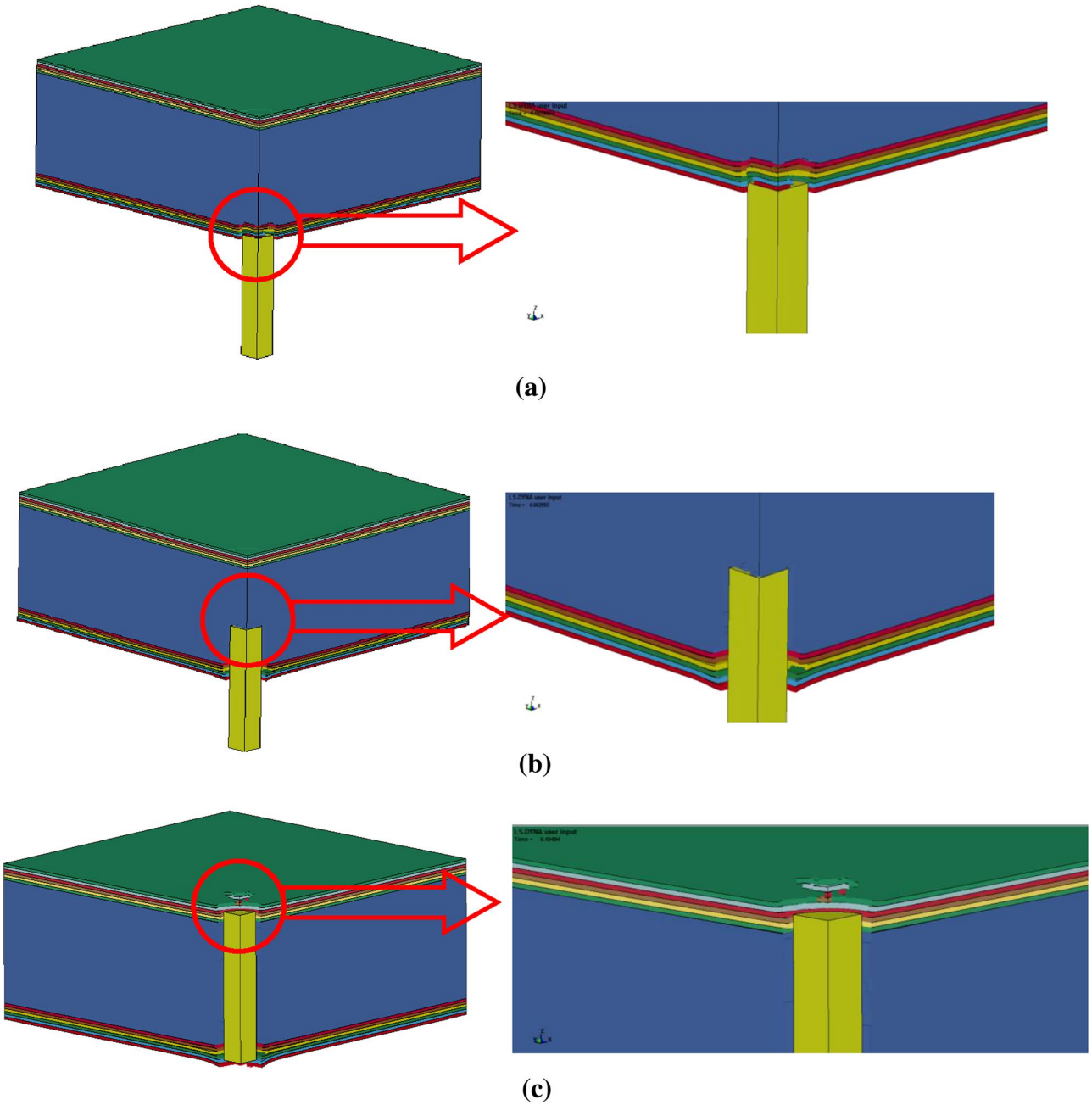

Fig. 8 Penetration of projectile into sandwich panel in LS-Dyna simulation. **a** Projectile penetration into front skin, **b** projectile penetration into foam core, **c** projectile penetration into back up skin

skins, and foam thickness are equal to 200, 1.75, and 25 mm, respectively. The ballistic limit velocity has been computed based on the global deformation failure model. It is evident that when the projectile's mass increases, with the constant values of projectile diameter, the ballistic limit velocity decreases. In addition, when the diameter of projectile increases the ballistic limit velocity increases.

Figure 13 shows the residual velocity versus the diameter of projectile D for different flat-ended projectile masses. It is evident that when the projectile's mass increases, considering the constant values of projectile diameter, the residual velocity increases. In addition, when the diameter of the projectile increases the residual velocity decreases.

Figure 14 illustrates the total energy absorbed by the composite skins of sandwich panel (E_{dcom}) and also different mechanisms of energy absorption including deformation (E_{def}), delamination (E_{del}), and fracture energy (E_{frac})

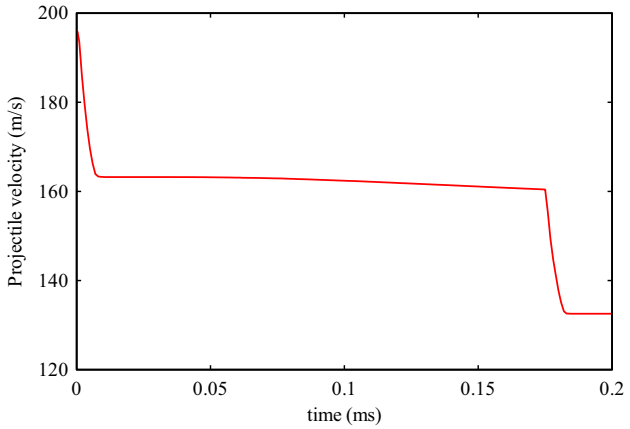

Fig. 9 The velocity-time history of projectile during perforation in LS-Dyna simulation

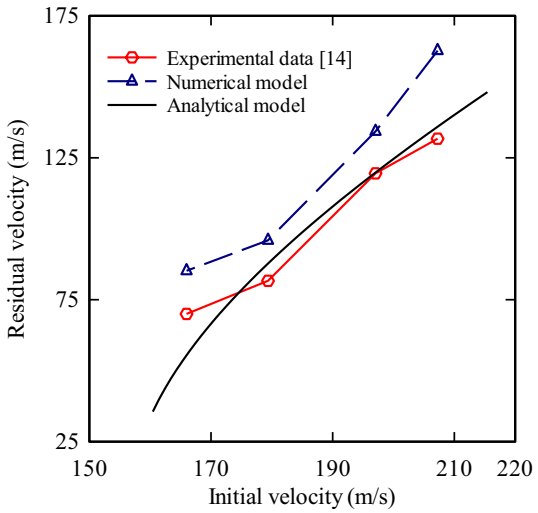

Fig. 10 Residual velocity versus initial velocity of projectile and comparison numerical and analytical model prediction with experimental results [13]

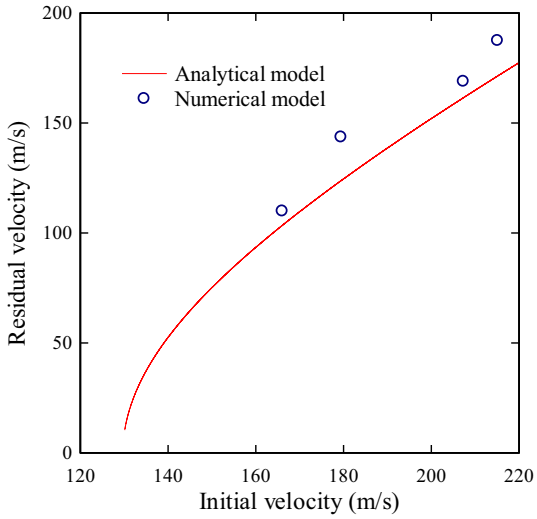

Fig. 11 Residual velocity versus initial velocity of projectile and comparison analytical model prediction with numerical model (carbon/epoxy skins and Divinycell H130 foam)

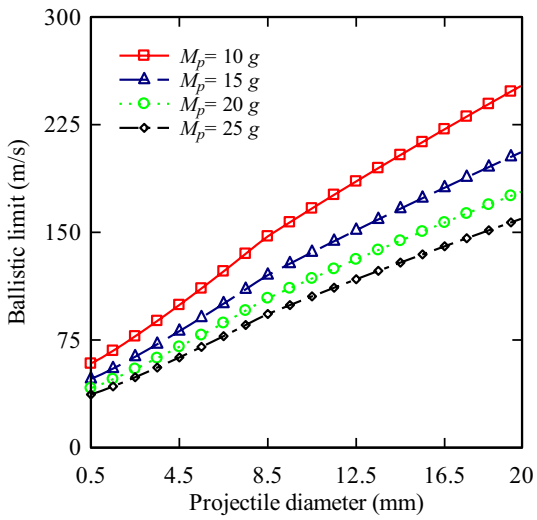

Fig. 12 Ballistic limit velocity versus projectile diameter for different projectile masses

computed by the new model versus the ratio of total composite skin thicknesses to the projectile diameter (T/D).

The diameter and mass of projectile are equal to 10.5 mm and 20.4 g. It is clear that increasing the composite skin thicknesses causes the absorbed energy enhances. In addition, it is obvious that the absorbed energy of skins due to deformation is more than the energy dissipated by the delamination and local failure. In addition, the energy dissipated by delamination and local failure of skins is approximately equal.

The absorbed energy by foam, composite skins, and sandwich panel versus the projectile diameter is presented in Fig. 15. Panel span, foam, and composite skin thicknesses are equal to 200, 25, and 3.25 mm, respectively. It is evident that when the projectile's diameter increases, the panel-absorbed energy increases. In addition, the foam-energy absorbed values are less than that of composite skin energy absorption. Therefore, the foam has low effects in the penetration resistance of sandwich panels. While the projectile diameter increases, foam effects in energy absorption by panel increase.

5 Conclusions

In this paper, a simple analytical model of high-velocity impact into the composite sandwich panels with

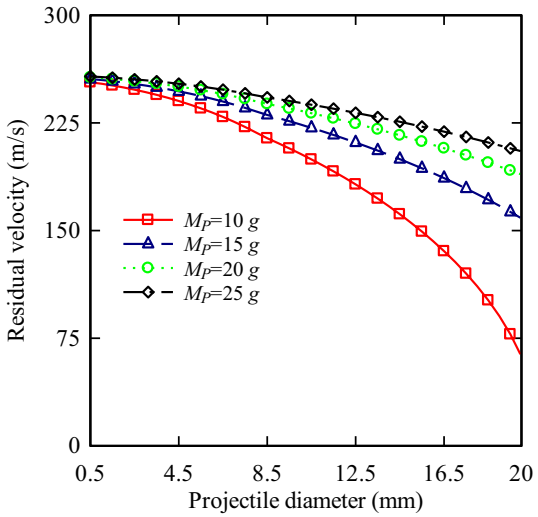

Fig. 13 Residual velocity versus projectile diameter for different projectile masses

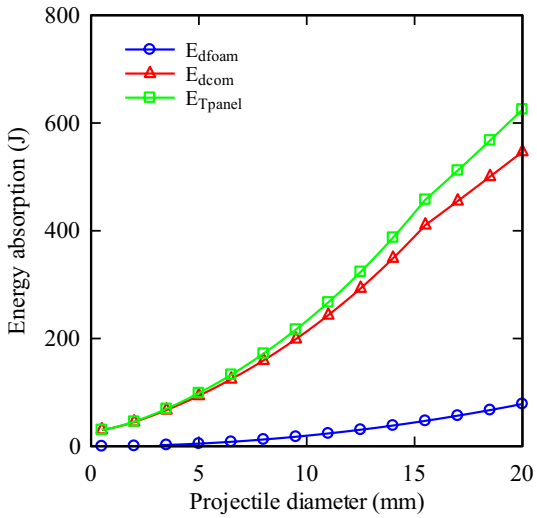

Fig. 15 Energy absorption by foam, composite skins, and sandwich panel versus projectile diameter

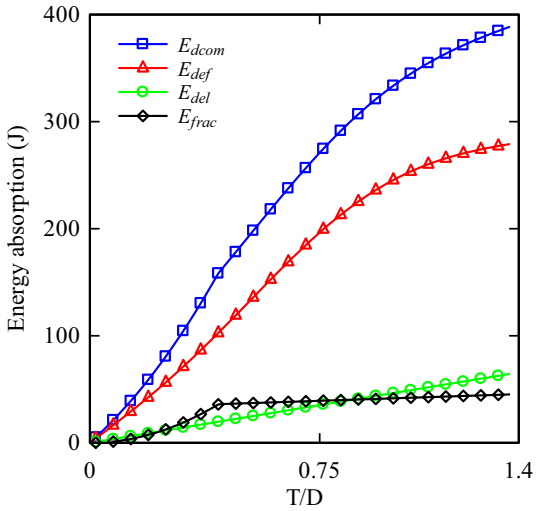

Fig. 14 Energy absorption by composite skins versus ratio of composite skins thickness to projectile diameter

honeycomb core has been developed. The residual and ballistic limit velocity of projectile computed by new model has an acceptable consistency with the Wen et al. [14] experimental results and F.E. simulation via LS-Dyna code.

According to the new model results, we can draw the following conclusions:

The analytical model, presented in this paper, is a simple and reliable way for predicting the penetration resistance of composite sandwich panels with foam core.

When the projectile's mass increases, with the constant values of projectile diameter, the ballistic limit velocity for perforation of sandwich panel decreases.

The value of energy absorption of composite skins due to deformation is more than the energy dissipated by delamination and local failure of laminates. In addition, the energy dissipated by delamination and local failure of skins is approximately equal.

The front and back-up composite skins are the main factor responsible for the energy absorption, while the effect of energy absorbed by the foam core is very low.

References

1. Ulven C, Vaidya UK, Hosur MV (2003) Effect of projectile shape during ballistic perforation of VARTM carbon/epoxy composite panels. Compos Struct 61(1–2):143–150
2. Wen HM (2000) Predicting the penetration and perforation of FRP laminates struck normally by projectiles with different nose shapes. Compos Struct 49(3):321–329
3. Wen HM (2001) penetration and perforation of thick FRP laminates. Compos Sci Technol 61:1163–1172
4. Naik NK, Shrirao P, Reddy BCK (2006) Ballistic impact behaviour of woven fabric composites: formulation. Int J Impact Eng 32(9):1521–1552
5. Feli S, Asgari MR (2011) Finite element simulation of ceramic/composite armor under ballistic impact. Compos B Eng 42(4):771–780
6. López-Puente J, Varas D, Loya JA, Zaera R (2009) Analytical modelling of high velocity impacts of cylindrical projectiles on carbon/epoxy laminates. Compos A Appl Sci Manuf 40(8):1223–1230
7. Mamivand M, Liaghat GH (2010) A model for ballistic impact on multi-layer fabric targets. Int J Impact Eng 37(7):806–812
8. Feli S, Yas MH, Asgari MR (2011) An analytical model for perforation of ceramic/multi-layered planar woven fabric targets by blunt projectiles. Compos Struct 93(2):548–556
9. Hoo Fatt MS, Park KS (2000) Perforation of honeycomb sandwich plates by projectiles. Compos A Appl Sci Manuf 31(8):889–899

10. Feli S, Namdari Pour MH (2012) An analytical model for composite sandwich panels with honeycomb core subjected to high-velocity impact. Compos B Eng 43(5):2439–2447
11. Lin C, Hoo Fatt MS (2006) Perforation of Composite Plates and Sandwich Panels under Quasi-static and Projectile Loading. J Compos Mater 40(20):1801–1840
12. Xie Z, Zheng Z, Yu J (2012) Localized indentation of sandwich panels with metallic foam core: analytical models for two types of indenters. Compos B Eng 44(1):212–217
13. Hoo Fatt MS, Sirivolu D (2010) A wave propagation model for the high velocity impact response of a composite sandwich panel. Int J Impact Eng 37(2):117–130
14. Wen H, Reddy T, Reid S, Soden P (1997) Indentation, penetration and perforation of composite laminate and sandwich panels under quasi-static and projectile loading. Key Eng Mater 141:501–552
15. Reddy T, Wen H, Reid S, Soden P (1998) Penetration and perforation of composite sandwich panels by hemispherical and conical projectiles. J Pressure Vessel Technol 120(2):186–194
16. Wu QG, Wen HM, Qin Y, Xin SH (2012) Perforation of FRP laminates under impact by flat-nosed projectiles. Compos B Eng 43(2):221–227
17. Shivakumar KN, Elber W, IIIg W (1985) Prediction of impact force and duration due to low velocity impact on circular composite laminates. Appl Mech 52(3):674–680
18. Davies GAO, Zhang X (1995) Impact damage prediction in carbon composite structures. Int J Impact Eng 16(1):149–170
19. Reid SR, Zhou G (2000) Impact behaviour of fibre-reinforced composite materials and structures. CRC Press, Boca Raton, FL
20. Gu B (2003) Analytical modeling for the ballistic perforation of planar plain-woven fabric target by projectile. Compos B Eng 34(4):361–371